




Measuring the Low-Energy Weak Mixing Angle with Supernova Neutrinos

Chun-Ming Yip ¹, Xu-Run Huang ^{1*}, Ming-chung Chu ¹, Qishan Liu ¹

¹Department of Physics and Institute of Theoretical Physics, The Chinese University of Hong Kong, Shatin, N.T., Hong Kong S.A.R., People's Republic of China.

*Corresponding author(s). E-mail(s): bryce.xr.huang@gmail.com;
Contributing authors: cmyip1999@gmail.com; mcchu@phy.cuhk.edu.hk;
qisliu@link.cuhk.edu.hk;

Abstract

The weak mixing angle θ_W is a fundamental parameter in the electroweak theory with a value running according to the energy scale, and its precision measurement in the low-energy regime is still ongoing. We propose a method to measure the low-energy $\sin^2\theta_W$ by taking advantage of Argo, a future ton-scale liquid argon dark matter detector, and the neutrino flux from a nearby core-collapse supernova (CCSN). We evaluate the expected precision of this measurement through the coherent elastic neutrino-nucleus scattering (CE ν NS) channel. We show that Argo is potentially capable of achieving a few percent determination of $\sin^2\theta_W$, at the momentum transfer of $q \sim 20$ MeV, in the observation of a CCSN within ~ 3 kpc from the Earth. Such a measurement is valuable for both the precision test of the electroweak theory and searching for new physics beyond the standard model in the neutrino sector.

1 Introduction

The weak mixing angle θ_W is one of the most fundamental parameters in the Standard Model (SM) of particle physics, which characterizes the mixing of vector bosons from the $SU(2)_L \times U(1)_Y$ symmetry [1]. Collider experiments in the last decades had achieved high precision measurements of $\sin^2\theta_W$ near the so-called ‘electroweak scale’ of ~ 100 GeV [2]. The value of $\sin^2\theta_W$ runs along with the energy scale where it is measured due to quantum effects, particularly at the next-to-leading-order. The SM prediction at zero momentum transfer $q = 0$ is $\sin^2\theta_W = 0.23863 \pm 0.00005$ under the modified minimal subtraction (\overline{MS}) renormalization scheme [2]. Experiments

are also performed to check this prediction. Nevertheless, the precise determination of $\sin^2\theta_W$ in the low-energy regime is still an ongoing issue [3].

Previous efforts can be categorized into the charged lepton and neutrino sectors. In the former, the Qweak Collaboration recently reported its result with a precision of $\pm 0.5\%$ at $q = 0.158$ GeV via the measurement of parity-violation asymmetry in a polarized electron scattering experiment [4], which agrees well with the SM prediction. In the low-energy regime, the most precise results to date are provided at $q \simeq 2.4$ MeV by the atomic parity violation (APV) experiments, but they turn out to be smaller than the SM prediction by $\sim 1.5\sigma$ [5, 6]. In the neutrino sector, an experimental anomaly (3σ) is reported by the NuTeV experiment, concerning the SM prediction

for neutrino-nucleon scatterings at $q \sim 1$ GeV [7]. At the MeV scale, the coherent elastic neutrino-nucleus scattering (CE ν NS) is a powerful probe, which was predicted theoretically in 1973 [8, 9] but only observed experimentally for the first time in 2017 [10]. In this interaction, the recoil of the nucleus is the only observable signature, which is very difficult to detect since it shows up with an extremely small kinetic energy. Hitherto observations have been achieved by the COHERENT collaboration using a cesium-iodide (CsI) detector [10] and a liquid argon detector [11], and by the Dresden-II experiment using a germanium detector [12]. The fresh detection of solar ^8B neutrinos on dark matter (DM) detectors, reported by the PandaX [13] and XENON [14] collaborations, are also conducted via the CE ν NS. Limited by the sparse data, an accurate extraction of $\sin^2\theta_W$ still requires further efforts (for recent progress, see Refs. [15, 16]). Meanwhile, the nature of neutrinos remains elusive. New physics beyond the SM may exist in the low-energy neutrino-nucleon interactions and shift the extracted value of $\sin^2\theta_W$ in these interactions [3, 17–19], e.g., neutrino non-standard interactions (NSIs) [20–22], neutrino charge properties [23], etc.. Any experimental constraints in this sector also render valuable information on searching for new physics beyond the SM.

Such a scientific potential stimulates further experimental and theoretical attention to the CE ν NS. Using low-energy neutrino fluxes from nuclear reactors or stopped-pion decays in accelerators, some terrestrial CE ν NS experiments are running, under construction, or being planned, e.g., CONUS [24], CONNIE [25], new COHERENT detectors [26], MINER [27], NEON [28], NUCLEUS [29], Ricochet [30], RED-100 [31], and so on [32]. Meanwhile, based on some of the above reactor neutrino experiments, the prospect of measuring the low-energy $\sin^2\theta_W$ has been discussed, e.g., a sub-1% extraction precision is found to be possible in ideal cases [33].

CE ν NS measurements can also be conducted using the low-energy neutrino flux from a galactic core-collapse supernova (CCSN). The first-ever supernova neutrino detection was done for SN 1987A, by the Kamiokande II, Irvine-Michigan-Brookhaven (IMB), and Baksan detectors [34–36]. Sophisticated CCSN simulations, in the meantime, have been performed by different groups to

predict the neutrino signals of CCSNe [37–40]. It is found that $\sim 10^{58}$ neutrinos, with mean energies of $\sim 10 - 20$ MeV, are released within a few seconds after a CCSN explosion occurs. Such a neutrino flux can be detected by large-scale DM detectors. For example, the sensitivity of future xenon and argon DM detectors to supernova neutrinos has been investigated, and $\gtrsim 10^2$ CE ν NS events are expected to be observed for a typical CCSN at 10 kpc from the Earth [41, 42]. Meanwhile, other dedicated large-scale neutrino observatories, such as Super-Kamiokande [43] (Hyper-Kamiokande [44]), DUNE [45], RES-NOVA [46, 47], JUNO [48], and so on [38, 49, 50], are capable of collecting a substantial number of supernova neutrino events, e.g., $\mathcal{O}(10^5)$ for a source at 10 kpc [38, 50]. So, a combined analysis of data from multiple detectors may potentially achieve a precise reconstruction of supernova neutrino energy spectrum for a nearby CCSN [51–56].

Measuring the low-energy $\sin^2\theta_W$ is feasible by taking advantage of the reconstructed supernova neutrino spectrum from large-scale neutrino observatories and the CE ν NS events in large-scale DM detectors. In this work, we estimate the potential of measuring the low-energy $\sin^2\theta_W$ with Argo, a proposed next-generation liquid argon DM detector [42, 57], in the observation of a nearby CCSN. This paper is organized as follows. In Sec. 2, we introduce the general properties of supernova neutrinos and 4 example fluxes obtained by numerical simulations. In Sec. 3, we present the detection prospect in Argo. The expected precision and relevant uncertainty analysis of the low-energy $\sin^2\theta_W$ measurement are shown in Sec. 4. Finally, we conclude in Sec. 5.

2 Supernova neutrino flux

In a real measurement, the neutrino flux can be determined by observations, including the direct measurements by dedicated neutrino observatories and outcomes from CCSN models which have been calibrated by multi-messenger observations. In this paper, we use neutrino fluxes from CCSN simulations in the literature. Thanks to tremendous progress in modeling CCSN phenomena in the last decades, modern hydrodynamic codes are capable of showing robust explosions in simulations [40, 58]. The supernova neutrino energy

spectrum of one species (ν_β in ν_e, ν_μ, ν_τ , and anti-particles) is well approximated by a quasi-thermal distribution (the so-called Garching formula [59, 60]) as a function of neutrino energy E_{ν_β} :

$$f_{\nu_\beta}(E_{\nu_\beta}) = C_\beta \left(\frac{E_{\nu_\beta}}{\langle E_{\nu_\beta} \rangle} \right)^{\alpha_\beta} \exp \left\{ -(\alpha_\beta + 1) \frac{E_{\nu_\beta}}{\langle E_{\nu_\beta} \rangle} \right\}, \quad (1)$$

where $\langle E_{\nu_\beta} \rangle$ is the mean neutrino energy, α_β is the shape parameter which controls the suppression of high energy tail, and the normalization constant C_β is given by

$$C_\beta = \frac{(\alpha_\beta + 1)^{\alpha_\beta + 1}}{\langle E_{\nu_\beta} \rangle \Gamma(\alpha_\beta + 1)} \quad (2)$$

for the species ν_β , with Γ denoting the gamma function. Neutrino flavor transitions [61] have no impact on our results since the CE ν NS is flavor-blind. The total neutrino flux on the Earth can be evaluated by summing over all neutrino species, i.e.,

$$\Phi(E_\nu) = \sum_\beta \frac{1}{4\pi d^2} \frac{E_{\nu_\beta}^{tot}}{\langle E_{\nu_\beta} \rangle} f_{\nu_\beta}(E_{\nu_\beta}) \quad (3)$$

as a function of neutrino energy E_ν regardless of species, with d being the distance of the CCSN and $E_{\nu_\beta}^{tot}$ the total energy emitted through one species. In practice, Eq. (1) is used to describe the energy spectrum of both the time-integrated flux as $f_{\nu_\beta}(E_{\nu_\beta})$, and the time-dependent flux as $f_{\nu_\beta}(E_{\nu_\beta}, t)$ with $\alpha_\beta(t)$ and $\langle E_{\nu_\beta}(t) \rangle$. Correspondingly, Eq. (3) can also describe the total differential flux $\Phi(E_\nu, t)$ with $\langle E_{\nu_\beta}(t) \rangle$ and $f_{\nu_\beta}(E_{\nu_\beta}, t)$, after replacing $E_{\nu_\beta}^{tot}$ with the neutrino luminosity $\mathcal{L}_{\nu_\beta}(t)$. The time-integrated flux is defined as $\Phi(E_\nu) \equiv \int \Phi(E_\nu, t) dt$.

Table 1 The CCSN models from the Garching group [37, 38]. The progenitor mass and nuclear EoS of each model are listed.

Model	Progenitor mass [M_\odot]	EoS
s11.2-S	11.2	Shen
s11.2-L	11.2	LS220
s27.0-S	27.0	Shen
s27.0-L	27.0	LS220

The neutrino fluxes from CCSN simulations depend not only on the properties of progenitor star (e.g., mass, compactness, etc. [62, 63]) but also on the nuclear matter equation of state (EoS) [64–66]. We use realistic values of $\alpha_\beta(t)$, $\langle E_{\nu_\beta}(t) \rangle$ and $\mathcal{L}_{\nu_\beta}(t)$ from 4 CCSN explosion models provided by the Garching group, considering the above factors. These models are listed in Table 1, and refer to Ref. [37, 38]. The temporal evolution of the neutrino spectral parameters is shown in Fig. 1 for the models s11.2-S and s27.0-L, where the former (latter) model results in the smallest (largest) expected number of event counts among the 4 models (see Sec. 3). Note that the time-integrated flux $\Phi(E_\nu)$ is already sufficient to compute the total number of CE ν NS events, and that is also what we can directly construct from the detection by other neutrino observatories. We further remark that the CCSN models can also be calibrated by multi-messenger observations, which provide more reliable information on the time-dependent supernova neutrino emission for a nearby CCSN explosion in the future.

3 Detection prospect in Argo

The primary purpose of conventional direct DM detectors is to search for nuclear recoils induced by galactic DM particles (e.g., the weakly interacting massive particles). The CE ν NS signals induced by solar neutrinos, reactor neutrinos, atmospheric neutrinos, the diffuse supernova neutrino background, and geoneutrinos will become an unavoidable background as the sensitivity of DM detectors approaches keV level [67, 68]. Conversely, these detectors can act as excellent low-energy neutrino observatories. The opportunity of observing supernova neutrinos has been investigated for large-scale DM detectors, e.g., liquid xenon detectors like XENONnT, DARWEN, and LZ [41, 69] as well as liquid argon detectors like DarkSide-20k and Argo [42]. In this section, we demonstrate how to obtain the expected CE ν NS event counts of the Argo experiment.

The Argo experiment is proposed as an extension of DarkSide-20k by the DarkSide Collaboration [42, 57]. It is assumed to have a dual-phase Liquid Argon Time Projection Chamber (LAr TPC) with an active mass of 362.7 tons (see, e.g., Ref. [42]). Such a dual-phase TPC is primarily filled with liquid argon and has a gaseous argon

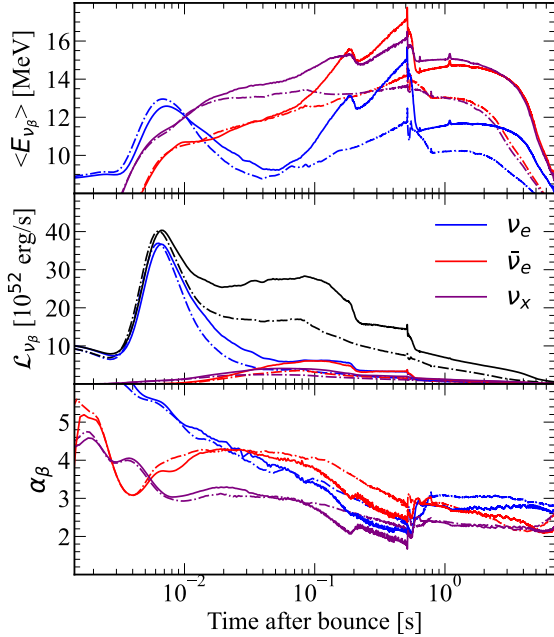


Fig. 1 Temporal evolution of supernova neutrino spectral parameters for the models s11.2-S (dashed-dotted lines) and s27.0-L (solid lines). ν_e , $\bar{\nu}_e$, and ν_x (ν_x denotes one of ν_μ , $\bar{\nu}_\mu$, ν_τ , and $\bar{\nu}_\tau$) are colored blue, red, and purple, respectively. Upper panel: neutrino mean energies $\langle E_{\nu_\beta} \rangle$. Middle panel: neutrino luminosities \mathcal{L}_{ν_β} . The total neutrino luminosities are also shown in black. Lower panel: shape parameter α_β . Note that the explosions of the displayed 1D CCSN models were artificially triggered at ~ 0.5 s after bounce and some kinks appear accordingly in the above curves, which do not lead to any significant perturbing consequences for the subsequent proto-neutron star cooling evolution [38].

phase on the top. When a CE ν NS event occurs in the instrumented volume, two measurable signals are produced, i.e., a prompt light pulse (S1) induced by scintillation in the liquid phase, and a delayed pulse (S2) associated with ionization electrons. The S2-only mode can achieve a lower energy threshold and a better detection efficiency than the S1-only or S1-S2 coincident modes for supernova neutrino detection [41, 42].

The differential cross section of CE ν NS in the SM, as a function of the neutrino energy E_ν and the nuclear recoil energy T , is given by [70–72]

$$\frac{d\sigma}{dT}(E_\nu, T) = \frac{G_F^2 M}{4\pi} Q_W^2 F_W^2(q) \left[1 - \frac{T}{E_\nu} - \frac{MT}{2E_\nu^2} \right], \quad (4)$$

where G_F is the Fermi coupling constant, M the mass of the target nucleus with Z (N) protons (neutrons), Q_W the weak charge of the target nucleus, and $F_W(q)$ the corresponding weak form factor. The momentum transfer q is given by $q^2 = 2ME_\nu^2 T / (E_\nu^2 - E_\nu T) \simeq 2MT$ for $E_\nu \gg T$. Note that Eq. 4 describes the interaction between a neutrino and a nucleus with spin-0 [71]. Natural argon is 99.6% ^{40}Ar with spin-0 [73], so we neglect the contributions from other isotopes. The mass of ^{40}Ar can be calculated via $M = Z \times m_p + N \times m_n - (Z + N) E_B$, with m_p (m_n) being the rest mass of proton (neutron) and $E_B = 8.595259$ MeV the binding energy per nucleon [74].

The weak charge of a nucleus Q_W is given by

$$Q_W = -2(Zg_V^p + Ng_V^n), \quad (5)$$

where the proton and neutron vector couplings are $g_V^p = 1/2 - 2\sin^2\theta_W$ and $g_V^n = -1/2$, respectively, at the tree level. The weak form factor $F_W(q)$ can be computed by

$$F_W(q) = -2 \frac{[Zg_V^p F_p(q) + Ng_V^n F_n(q)]}{Q_W}, \quad (6)$$

where $F_{n(p)}(q)$ is the neutron (proton) form factor. We adopt the Helm parametrization [75, 76] since it is very successful in analyzing electron scattering form factors [77–79] and has also been used in previous CE ν NS studies [80–82]. It has the form as

$$F_i(q) = 3 \frac{j_1(qR_{0,i})}{qR_{0,i}} e^{-q^2 s^2/2}, \quad (7)$$

where $i = p, n$ labels the form factor associated with proton and neutron, respectively, and $j_1(x) = \sin x/x^2 - \cos x/x$ is the spherical Bessel function of order one. The diffraction radius $R_{0,i}$ is related to the root-mean-squared (rms) radius R_i by

$$R_i^2 = \frac{3}{5} R_{0,i}^2 + 3s^2, \quad (8)$$

with s quantifying the surface thickness. We adopt the value $s = 0.9$ fm, following Ref. [82]. R_i is associated with the point-nucleon distribution radius R_i^{point} and the radius of nucleon $\langle r_i^2 \rangle^{1/2}$, i.e.,

$$R_i^2 = (R_i^{\text{point}})^2 + \langle r_i^2 \rangle. \quad (9)$$

The radius of a proton equals its charge radius and has the value of $\langle r_p^2 \rangle^{1/2} = 0.8414(19)$ fm [83]. For neutron, we assume $\langle r_n^2 \rangle^{1/2} \simeq \langle r_p^2 \rangle^{1/2}$, which is supported by the neutron magnetic radius measurement [84]. Electron scattering experiments have made precise measurements on the charge radius of a nucleus (R_c), which is given by [85, 86]

$$R_c^2 = (R_p^{\text{point}})^2 + \langle r_p^2 \rangle + \frac{N}{Z} \langle r_n^2 \rangle_c, \quad (10)$$

with $\langle r_n^2 \rangle_c = -0.1161(22)$ fm² [84] being the squared charge radius of a neutron. For ⁴⁰Ar, it is measured as $R_c = 3.4274 \pm 0.0026$ fm [87, 88]. As a consequence, we obtain the value of R_p as

$$R_p = 3.448 \pm 0.003 \text{ fm}. \quad (11)$$

On the other hand, the neutron rms radius is experimentally unknown [89], and different nuclear models would give different predictions (see, e.g., Table I in Ref. [82]). Theoretical predictions indicate that R_n^{point} is universally larger than R_p^{point} by 0.08 – 0.11 fm for ⁴⁰Ar [82]. We take such an assumption:

$$R_n \simeq R_p + 0.1 \text{ fm}. \quad (12)$$

It should be further pointed out that the neutron form factors at $\mathcal{O}(10)$ MeV are not sensitive to uncertainties of neutron distributions in nuclei, especially for light nuclei like ⁴⁰Ar. We check it by varying $R_n - R_p$ by $\pm 20\%$ and the resulting CE ν NS event counts only deviate by about $\mp 0.1\%$ for the 4 CCSN models aforementioned.

We estimate the number of expected events \mathcal{N} in Argo by the expression

$$\mathcal{N} = N_{\text{Ar}} \int dE_\nu \mathcal{E}(E_\nu) \int_{T_{\text{min}}}^{T_{\text{max}}} dT \frac{d\sigma}{dT}(E_\nu, T) \Phi(E_\nu). \quad (13)$$

Here, $N_{\text{Ar}} = N_A m_{\text{det}} / M_{\text{Ar}}$ denotes the number of Ar atoms contained in the active volume of the detector, with N_A being the Avogadro constant, m_{det} the active mass of the detector, and $M_{\text{Ar}} = 39.96$ g/mol the molar mass of argon. We consider the E_ν -dependent detection efficiency $\mathcal{E}(E_\nu)$, which is evaluated in the range of [3, 100] ionization electrons (see Fig. 4 in Ref. [42]). This detection efficiency is preferred in the study of supernova neutrino detection by DarkSide-20k

and Argo, to suppress the single-electron background and the ³⁹Ar events [42]. When integrating over T , an energy threshold of $T_{\text{min}} = 0.46$ keV is considered, since it has been proven as feasible by DarkSide-50 [90] and also applied for Argo in Ref. [42]. For the scattering between a Ar nucleus and an incoming neutrino with an energy E_ν , $T_{\text{max}} = 2E_\nu^2 / (M_{\text{Ar}} + 2E_\nu)$. The integration over E_ν starts from 1 MeV, where $\mathcal{E}(E_\nu)$ already decreases to zero, and ends at 60 MeV, which is high enough for the energy spectrum (Eq. 1) to almost fade out. The scattering rate $d\mathcal{N}/dt$ can also be computed by Eq. (13) if we replace $\Phi(E_\nu)$ with $\Phi(E_\nu, t)$.

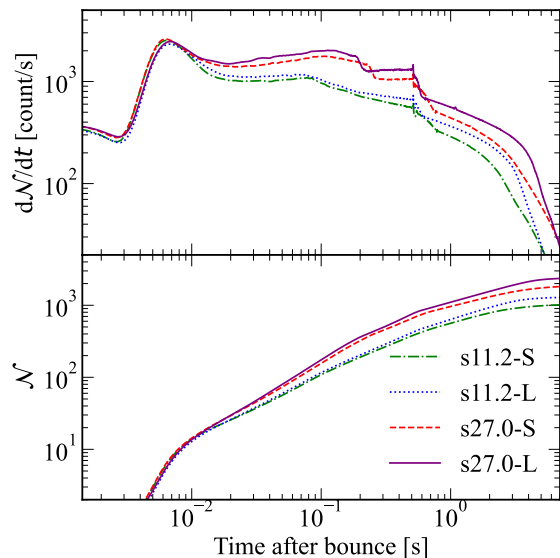


Fig. 2 Expected event counts of CE ν NS in Argo for the 4 models, evaluated at $d = 10$ kpc. Upper panel: Scattering rate $d\mathcal{N}/dt$. Lower panel: cumulative event counts \mathcal{N} over time.

Fig. 2 shows the scattering rate ($d\mathcal{N}/dt$) and the corresponding cumulative event counts for the 4 CCSN models, with the $\sin^2\theta_W$ in the SM at $d = 10$ kpc. The cumulative event counts \mathcal{N} are calculated to be 1012, 1284, 1820, and 2357 for the 4 CCSN models presented in Table 1, respectively, at 7 s after bounce and saturate afterward. More events are recorded for the models s27.0-S and s27.0-L with heavier progenitors. We also find that about half of the events are recorded within the first second after the bounce.

4 Low energy weak mixing angle sensitivity

4.1 Statistical analysis

To assess the precision of measuring $\sin^2 \theta_W$, we perform a χ^2 analysis, assuming that the number of observed events by Argo is $\mathcal{N}_{\text{obs}} = \mathcal{N}_{\text{true}} - \mathcal{N}_{\text{bias}}$, where $\mathcal{N}_{\text{true}}$ is the actual number of total CE ν NS interactions and $\mathcal{N}_{\text{bias}}$ is the number of unresolved interactions due to event pile-up (see later contents for more detailed discussions). Following Refs. [33, 72], we consider the chi-squared function

$$\chi^2 = \frac{(\mathcal{N}_{\text{obs}}^{\text{SM}} - \mathcal{N}_{\text{obs}}^{\text{th}})^2}{\sigma_{\text{stat}}^2 + \sigma_{\text{syst}}^2}. \quad (14)$$

Here, $\mathcal{N}_{\text{obs}}^{\text{SM}}$ denotes the number of observed events computed with the SM value of $\sin^2 \theta_W$ at zero momentum transfer, i.e., $\sin^2 \theta_W = 0.23863$ [2], while $\mathcal{N}_{\text{obs}}^{\text{th}}$ varies according to the value of $\sin^2 \theta_W$. We divide the uncertainty estimation into two parts, i.e., a pure statistical uncertainty $\sigma_{\text{stat}} = \sqrt{\mathcal{N}_{\text{obs}}^{\text{SM}}}$ and a systematic error σ_{syst} . In this section, we attempt to draw an estimation based on the current limited knowledge of σ_{syst} . Firstly, due to the ultra-high event rate and limitation from the time resolution of LAr TPC, the event pile-up will become inevitable for a nearby target. This will reduce the total count collected in Argo and introduce a systematic uncertainty. Secondly, the energy spectra of supernova neutrinos are measured with an uncertainty, and it introduces an uncertainty on the expected number of events in Argo. This uncertainty will be more pronounced for a far target. The total systematic error of the low-energy $\sin^2 \theta_W$ measurement considering the above two types of uncertainties can be written as $\sigma_{\text{syst}}^2 = \sigma_{\text{bias}}^2 + \sigma_{\text{flux}}^2$. Here, σ_{bias} denotes the uncertainty in event pile-up estimation in Argo; σ_{flux} denotes the flux uncertainty of expected events in Argo, which originates from the uncertainty of the extracted supernova neutrino flux σ_ν in other detectors. Nonetheless, there may also exist more uncertainties from other sources, e.g., the high-order corrections to the cross-section, the configuration of the Argo detector, and so on. In this section, we only consider the previous two types of uncertainties and leave a comprehensive

uncertainty evaluation to a real measurement in the future.

According to the study based on DarkSide-50 [91], the observed S2 signal in a dual-phase LAr TPC is a pulse with a width of $\sim 10 \mu\text{s}$ (or a FWHM of $\sim 5 \mu\text{s}$). When an intense neutrino flux from a nearby source comes into the LAr TPC, a large number of interactions occur within a short period of time, and some S2 pulses may overlap with each other. Such a phenomenon will reduce the total number of observed events by a bias number $\mathcal{N}_{\text{bias}}$. Meanwhile, $\mathcal{N}_{\text{bias}}$ will get a value randomly in the detection according to a probability distribution. To evaluate $\mathcal{N}_{\text{bias}}$ and its uncertainty, we use the Monte Carlo method to study the pile-up issue, which was also used in dual-phase xenon TPCs in Ref. [41]. We adopt the assumption that two S2 signals are distinguishable only if the spacing from the start of one pulse to the start of the next is larger than $10 \mu\text{s}$. Otherwise, these two close S2 signals will be combined as one. The expected events are distributed randomly in time according to the scattering rate dN/dt and uniformly throughout the TPC. Argo is assumed to have a height of 5 m and a drift velocity of $0.93 \text{ mm}/\mu\text{s}$ [42]. We also take into account the time delay due to the drifting of ionization electrons. With the above setup, a set of Monte Carlo simulations is performed, which consists of 3×10^4 individual mock triggers for each d . After that, we count the number of unresolved events in each trigger and obtain a histogram of $\mathcal{N}_{\text{bias}}$ for this dataset. Finally, the mean value $\langle \mathcal{N}_{\text{bias}} \rangle$ and uncertainty σ_{bias} can be extracted from the histogram. The Monte Carlo simulation results with $\sin^2 \theta_W = 0.23863$ are displayed in Fig. 3. As d decreases, the mean portion of pile-up events $\langle \mathcal{N}_{\text{bias}} \rangle / \mathcal{N}_{\text{true}}$ increases, but the relative 1σ variation $\sigma_{\text{bias}} / \mathcal{N}_{\text{true}}$ decreases. This is generic for all 4 CCSN models. The magnitude of σ_{bias} grows to ~ 100 when d approaches 1 kpc, which is $\sim 0.1\%$ of $\mathcal{N}_{\text{true}}$ in all models.

The prediction of $\mathcal{N}_{\text{bias}}$ depends on the CCSN model (e.g., the progenitor mass) and d , while σ_{bias} is less affected by these factors according to Fig. 3. In a real measurement, the multi-messenger observation of a nearby CCSN will be used to calibrate the CCSN model, and also to measure d (further discussions can be found in Sec. 4.2). Hence, we only consider the distance dependence now. We remark that, technically speaking, two S2

signals with a spacing smaller than $10\ \mu\text{s}$ can still be distinguished if the S2 pulse shapes get read out in a real measurement [91]. We also test the case of shrinking the criterion of resolving two successive events from $10\ \mu\text{s}$ to $5\ \mu\text{s}$ in the Monte Carlo simulations. Using the new criterion, $\langle\mathcal{N}_{\text{bias}}\rangle/\mathcal{N}_{\text{true}}$ is universally shifted down by a factor of $\sim 1/2$ at $d \gtrsim 3\ \text{kpc}$ in all models, and by a factor of $\sim 1/3$ at $d \sim 1\ \text{kpc}$. Another way to avoid a large portion of pile-up events is to only consider the cooling phase where the neutrino luminosity is less intense (e.g., $t \gtrsim 1\ \text{s}$ for the models in Fig. 1). Our simulations find that the mean portions of pile-up events are reduced by $\sim 50\%$ when only the cooling phases are considered.

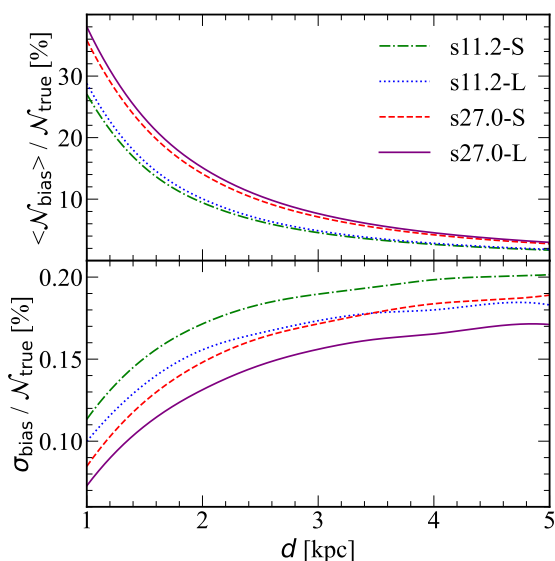


Fig. 3 Simulated event pile-up in Argo with $\sin^2\theta_W = 0.23863$. For each set of Monte Carlo simulations at a certain value of d , 3×10^4 individual mock triggers are generated. Upper panel: Mean portion of pile-up events $\langle\mathcal{N}_{\text{bias}}\rangle/\mathcal{N}_{\text{true}}$ (in percentage). Lower panel: 1σ variation of pile-up events $\sigma_{\text{bias}}/\mathcal{N}_{\text{true}}$.

Another issue is the uncertainty in the number of expected events in Argo. Although the time-dependent supernova neutrino fluxes are used to calculate the total number of expected counts in Eq. (14), the time-integrated neutrino fluxes should be used in a real measurement. They are expected to be measured by large-scale neutrino observatories in parallel to Argo. That is, by

analyzing the data from one detector or a combination of multiple detectors, parameters of the time-integrated neutrino spectra can be reconstructed via various methods (see, e.g., Refs. [51–56]). We firstly estimate the uncertainty of the extracted supernova neutrino flux σ_ν (in percentage) in other detectors according to the parameter extraction precision of all flavors in a Bayesian approach [56]. The 2σ extraction precision for the observation of a 10 kpc target is presented in Table 3 of Ref. [56], for both normal mass ordering (NMO) and inverted mass ordering (IMO). We first calculate the total neutrino spectra according to the 2σ parameter space and find the upper and lower boundaries. Then, we integrate the neutrino spectra to get the total numbers of neutrinos associated with the most probable spectrum as well as the two boundaries. The 2σ flux uncertainty can thus be estimated as the difference in total numbers of neutrinos (in percentage) between the most probable spectrum and the two boundaries. We find that $\sigma_\nu \simeq 14.1(13.1)\%$ at $d = 10\ \text{kpc}$ assuming NMO (IMO). Furthermore, the authors of Ref. [56] also tested the distance effect by assuming a closer source, e.g., $d = 5\ \text{kpc}$, and they find that the precisions are improved by about 40 – 50% among almost all parameters. Their results indicate that the reconstruction uncertainty is currently dominated by the statistics. Consequently, we make such an assumption: $\sigma_\nu \propto 1/\sqrt{\mathcal{N}_\nu} \propto d$ since the total number of supernova neutrinos on the Earth is $\mathcal{N}_\nu \propto 1/d^2$. While $\mathcal{N}_{\text{true}}^{\text{th}} \propto \mathcal{N}_\nu$ and $\mathcal{N}_{\text{bias}}^{\text{th}}$ is also related to \mathcal{N}_ν , we can estimate the flux uncertainty of expected events σ_{flux} in Argo according to the uncertainty of the extracted supernova neutrino flux σ_ν in other detectors evaluated above. Thus, we adopt $\sigma_{\text{flux}} \simeq \mathcal{N}_{\text{obs}}^{\text{th}} \times 14.1\% \times (d/10\ \text{kpc})$ assuming NMO. To test such an estimate, we perform an additional set of Monte Carlo simulations for the model s27.0-L, following the aforementioned setting, and vary $\mathcal{N}_{\text{true}}$ by $\pm 10\%$. The resulting variation in \mathcal{N}_{obs} is about $\pm 10(7)\%$ at $d = 5(1)\ \text{kpc}$, smaller than the variation in $\mathcal{N}_{\text{true}}$ itself at small d . Therefore, we remark that the above expression of σ_{flux} may slightly overestimate the flux extraction uncertainty for a very close source. The caveat is that the assumption of $\sigma_\nu \propto d$ may not work for a very close source, since other systematic errors may overwhelm the statistical error.

Finally, we obtain the total systematic error of the low-energy $\sin^2\theta_W$ measurements by $\sigma_{\text{syst}}^2 = \sigma_{\text{bias}}^2 + \sigma_{\text{flux}}^2$. We evaluate the expected sensitivity of Argo to the variation in $\sin^2\theta_W$ using Eq. (14). The sensitivity curves at a few benchmark values of d are shown in Fig. 4 for the model s27.0-L as an example. NMO is assumed when evaluating σ_{flux} , and a similar result is obtained when IMO is assumed. Currently, σ_{flux} is the most significant source of uncertainty for these benchmark values of d . The expected precision of the low-energy $\sin^2\theta_W$ measurement is higher for a smaller d due to the proportionality of σ_{flux} to d . In particular, a theoretical precision of 2.8(1.3)% can be achieved at $d = 3(1)$ kpc. Note that the corresponding curves for different SN models are nearly identical. We further remark that these results should generally be considered as upper limits of the precision due to incomplete uncertainty evaluation.

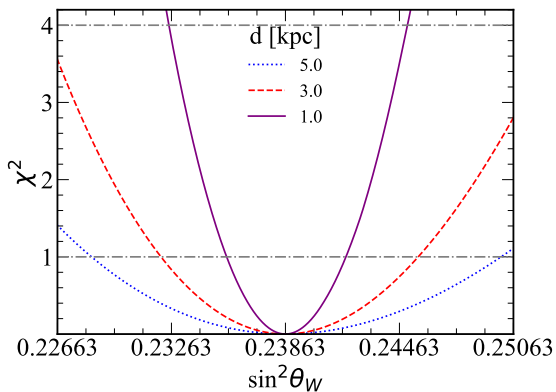


Fig. 4 Expected sensitivity of Argo to the variation in low-energy $\sin^2\theta_W$ from the SM value of 0.23863, at a few benchmark values of d . The model s27.0-L and NMO are assumed.

4.2 Discussions

It is meaningful to compare our results with other approaches [92]. Fig. 5 shows the comparison between the expected precision of low-energy $\sin^2\theta_W$ measurement by Argo, as indicated in Fig. 4, and those of other experiments. Especially, we would like to compare our results with the expected sensitivities of the CONNIE, MINER, and RED-100 reactor neutrino experiments [33], which also rely on the detection of $\text{CE}\nu\text{NS}$ events.

While the optimistic precision of these experiments is expected to be $\sim 1\%$, comparable precision ($\lesssim 3\%$) may also be achievable for Argo if the supernova neutrino flux from a CCSN at $d \lesssim 3$ kpc is available.

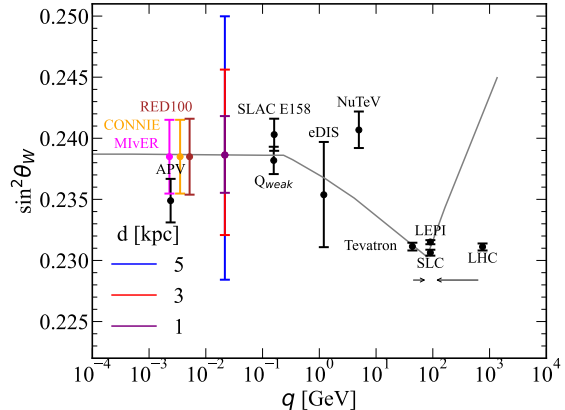


Fig. 5 Comparison between the expected precision of low-energy $\sin^2\theta_W$ measurement by Argo and other approaches [92] at different momentum transfers q . In particular, the optimistic expected sensitivities of the CONNIE, MINER, and RED-100 reactor neutrino experiments [33] are highlighted in colors.

The measurement of low-energy $\sin^2\theta_W$ also sheds light on searching for new physics. For example, the interactions between low-energy neutrinos and nucleons could potentially involve new physics beyond the SM, which can be described by the neutrino NSIs [16, 93]. As a result, these NSIs could introduce an effective shift in the SM value of $\sin^2\theta_W$, which can be identified by Argo due to the modification in the differential cross section of $\text{CE}\nu\text{NS}$. By considering the neutrino NSIs with u and d quarks described by the effective Lagrangian [17, 94, 95], the weak charge Q_W and the weak Form factor of ^{40}Ar are modified [96]. Based on the anticipated high-precision measurements of $\sin^2\theta_W$ at low energies, as illustrated in Fig. 4, the sensitivity to the NSI parameters, such as $\varepsilon_{\alpha\alpha}^{uV}$ and $\varepsilon_{\alpha\alpha}^{dV}$, could reach the range of $(-0.006, 0.006)$ at a 90% confidence level ($\chi^2 = 2.71$) for a CCSN event located at $d \sim 3$ kpc. Such an improvement in sensitivity enhances the precision of constraining the neutrino NSI parameters by approximately one order of magnitude compared to the first COHERENT data [97–101].

We remark that the supernova neutrino flux is crucial in our evaluation. When we evaluate the total number of CE ν NS events, we can simply use the time-integrated neutrino flux reconstructed from other observations. The time-dependent neutrino flux from a well-calibrated supernova simulation, nevertheless, would be necessary for the estimation of pile-up events for a close source. In this work, we adopt 4 CCSN models to estimate the event pile-up in Argo detector. The results (see Fig. 3) indicate that the number of unresolved events depends on the progenitor mass, nuclear EoS and source distance. Unlike the progenitor mass and source distance that will be measured via multi-messenger observations for a nearby target [102, 103], the nuclear EoS properties remain uncertain and required further determinations [104–106]. For example, the value of nuclear matter incompressibility is reported to be 240 ± 20 MeV from isoscalar giant monopole resonance experiment, and is adopted in various relevant studies [107–113]. The incompressibility of the LS220 and Shen EoS, employed by these CCSN models, is 220 and 281 MeV, respectively [114, 115]. Such choices represent two extremes with respect to the aforementioned experimental constraint. The difference in pile-up portion $\langle \mathcal{N}_{\text{bias}} \rangle / \mathcal{N}_{\text{true}}$ between the CCSN models using the LS220 and Shen EoSs increases from 0.11(0.22)% at $d = 5$ kpc to 1.73(2.19)% at $d = 1$ kpc for the models with progenitor mass being 11.2 (27.0) M_{\odot} (see Fig. 3). Hence, we believe that the influence of the nuclear EoS uncertainties on our results may be noticeable at a very small d , and further analysis is required to study its impacts quantitatively. Note that, however, different values and confidence ranges of incompressibility are obtained using other approaches (see, e.g., Refs. [116–118]). It is worth paying attention to the latest progress on constraining nuclear EoS through astrophysical observations and nuclear experiments [119–123]. We expect an even smaller uncertainty from the nuclear EoS once the supernova simulation is further calibrated by future observations and experiments.

Another issue is the occurrence of the next galactic CCSN. A list of 31 CCSN candidates within 1 kpc from the Earth is suggested in Ref. [102]. More candidates can be expected within a range of 5 kpc. Meanwhile, the supernova rate is estimated to be 1.63 ± 0.46 per century

for the Milky Way Galaxy [124]. Nonetheless, it has been 420 years since the last observed galactic supernova, i.e., the Kepler supernova in 1604 [125], and we can tell that no galactic supernova has occurred for at least 38 years, according to the neutrino detection, since the extra-galactic SN 1987A. Among the last 1,000 years, only 6 galactic supernovae were recorded: Lupus at 2.2 kpc in 1006, Crab at 2.0 kpc in 1054, 3C 58 at 2.6 kpc in 1181, Tycho at 2.4 kpc in 1572, Kepler at 4.2 kpc in 1604, and Cas A at 2.92 kpc in 1680, all happened within 5 kpc from the Earth. 4 of these events out of 6, namely Crab, 3C 58, Kepler, and Cas A, were considered to be CCSNe [126]. The next galactic supernova seems to be imminent and possible to be a CCSN. It is meaningful to get prepared to catch such an once-in-a-life-time chance.

5 Conclusions

We study the low-energy $\sin^2 \theta_W$ measurement by Argo in the observation of a nearby CCSN explosion, through the CE ν NS interaction. A galactic CCSN event provides an intense neutrino flux with a mean energy of $\sim 10 - 20$ MeV, and will be observed by both Argo and other dedicated neutrino observatories. Given the great progress in neutrino detection in the last decades, the next nearby CCSN will be well observed and also be used to calibrate the CCSN simulations. The Argo detector can collect the CE ν NS signals when those MeV neutrinos scatter off the argon nuclei, providing a way to extract the value of low-energy $\sin^2 \theta_W$. We further consider the systematic uncertainties due to the flux extraction of supernova neutrinos and event pile-up, and find that a precision of $\lesssim 3\%$ is potentially possible at a supernova distance $d \lesssim 3$ kpc. Such a precision is comparable to the optimistic expected sensitivity of ongoing terrestrial measurements, including the CONNIE, MINER, and RED-100 reactor neutrino experiments, in the similar momentum transfer (see Fig. 5). Our analysis of the systematic uncertainties can provide valuable information for the experimentalists to improve their strategy in the observation of the next nearby CCSN. However, the caveat is that this result should be taken as an upper limit of the precision due to the currently incomplete uncertainty estimation. We leave the detailed analysis of the systematic uncertainties in a real measurement to future work. Note that

Argo is more suitable for such a measurement among different large-scale CE ν NS detectors since the uncertainty from the argon nucleus structure is relatively small compared to that of the heavier nuclei, such as xenon and lead which constitute the active targets of PandaX [127] / XENONnT [128] and RES-NOVA [46], respectively.

The precise measurement of the low-energy $\sin^2 \theta_W$ is important for the precision test of the SM. Any deviation may provide a hint to new physics, especially in the neutrino sector where the existence of new physics has already been proven by neutrino oscillation experiments. Specifically, such a measurement can be used to constrain the neutrino NSI parameters. Recently, the PandaX [13] and XENON [14] collaborations reported the first detection of solar ^8B neutrinos by direct DM detectors, through the CE ν NS channel. Since the solar ^8B neutrinos have been well-studied, future multi-ton scale DM detectors may also provide excellent opportunities to determine the low-energy $\sin^2 \theta_W$ via such measurements.

Acknowledgements. We acknowledge Hans-Thomas Janka, Daniel Kresse, Lorenz Hüdepohl, and Alessandro Mirizzi for granting access to the Garching Core-Collapse Supernova Archive (<https://wwwmpa.mpa-garching.mpg.de/ccsnarchive>). We thank Tianyu Zhu and Kaixuan Ni for the discussions on DM detectors. This work is partially supported by grants from the Research Grant Council of the Hong Kong Special Administrative Region, China (Project Nos. 14300320 and 14304322). This material is based upon work supported by the National Science Foundation under Grant AST-2316807.

References

- [1] Weinberg, S.: A Model of Leptons. *Phys. Rev. Lett.* **19**, 1264–1266 (1967) <https://doi.org/10.1103/PhysRevLett.19.1264>
- [2] Workman, R.L., *et al.*: Review of Particle Physics. *PTEP* **2022**, 083–01 (2022) <https://doi.org/10.1093/ptep/ptac097>
- [3] Kumar, K.S., Mantry, S., Marciano, W.J., Souder, P.A.: Low Energy Measurements of the Weak Mixing Angle. *Ann. Rev. Nucl. Part. Sci.* **63**, 237–267 (2013) <https://doi.org/10.1146/annurev-nucl-102212-170556> [arXiv:1302.6263](https://arxiv.org/abs/1302.6263) [hep-ex]
- [4] Androić, D., *et al.*: Precision measurement of the weak charge of the proton. *Nature* **557**(7704), 207–211 (2018) <https://doi.org/10.1038/s41586-018-0096-0> [arXiv:1905.08283](https://arxiv.org/abs/1905.08283) [nucl-ex]
- [5] Dzuba, V.A., Berengut, J.C., Flambaum, V.V., Roberts, B.: Revisiting parity non-conservation in cesium. *Phys. Rev. Lett.* **109**, 203003 (2012) <https://doi.org/10.1103/PhysRevLett.109.203003> [arXiv:1207.5864](https://arxiv.org/abs/1207.5864) [hep-ph]
- [6] Roberts, B.M., Dzuba, V.A., Flambaum, V.V.: Parity and Time-Reversal Violation in Atomic Systems. *Ann. Rev. Nucl. Part. Sci.* **65**, 63–86 (2015) <https://doi.org/10.1146/annurev-nucl-102014-022331> [arXiv:1412.6644](https://arxiv.org/abs/1412.6644) [physics.atom-ph]
- [7] Zeller, G.P., *et al.*: A Precise Determination of Electroweak Parameters in Neutrino Nucleon Scattering. *Phys. Rev. Lett.* **88**, 091802 (2002) <https://doi.org/10.1103/PhysRevLett.88.091802> [arXiv:hep-ex/0110059](https://arxiv.org/abs/hep-ex/0110059). [Erratum: *Phys. Rev. Lett.* **90**, 239902 (2003)]
- [8] Freedman, D.Z.: Coherent Neutrino Nucleus Scattering as a Probe of the Weak Neutral Current. *Phys. Rev. D* **9**, 1389–1392 (1974) <https://doi.org/10.1103/PhysRevD.9.1389>
- [9] Freedman, D.Z., Schramm, D.N., Tubbs, D.L.: The Weak Neutral Current and Its Effects in Stellar Collapse. *Ann. Rev. Nucl. Part. Sci.* **27**, 167–207 (1977) <https://doi.org/10.1146/annurev.ms.27.120177.001123>
- [10] Akimov, D., *et al.*: Observation of Coherent Elastic Neutrino-Nucleus Scattering. *Science* **357**(6356), 1123–1126 (2017) <https://doi.org/10.1126/science.aao0990> [arXiv:1708.01294](https://arxiv.org/abs/1708.01294) [nucl-ex]
- [11] Akimov, D., *et al.*: First Measurement of Coherent Elastic Neutrino-Nucleus Scattering on Argon. *Phys. Rev.*

- Lett. **126**(1), 012002 (2021) <https://doi.org/10.1103/PhysRevLett.126.012002> arXiv:2003.10630 [nucl-ex]
- [12] Colaresi, J., Collar, J.I., Hossbach, T.W., Lewis, C.M., Yocum, K.M.: Measurement of Coherent Elastic Neutrino-Nucleus Scattering from Reactor Antineutrinos. Phys. Rev. Lett. **129**(21), 211802 (2022) <https://doi.org/10.1103/PhysRevLett.129.211802> arXiv:2202.09672 [hep-ex]
- [13] Bo, Z., *et al.*: First Indication of Solar B8 Neutrinos through Coherent Elastic Neutrino-Nucleus Scattering in PandaX-4T. Phys. Rev. Lett. **133**(19), 191001 (2024) <https://doi.org/10.1103/PhysRevLett.133.191001> arXiv:2407.10892 [hep-ex]
- [14] Aprile, E., *et al.*: First Indication of Solar B8 Neutrinos via Coherent Elastic Neutrino-Nucleus Scattering with XENONnT. Phys. Rev. Lett. **133**(19), 191002 (2024) <https://doi.org/10.1103/PhysRevLett.133.191002> arXiv:2408.02877 [nucl-ex]
- [15] Pandey, V.: Recent progress in low energy neutrino scattering physics and its implications for the standard and beyond the standard model physics. Prog. Part. Nucl. Phys. **134**, 104078 (2024) <https://doi.org/10.1016/j.pnpnp.2023.104078> arXiv:2309.07840 [hep-ph]
- [16] Cadeddu, M., Dordei, F., Giunti, C.: A view of coherent elastic neutrino-nucleus scattering. EPL **143**(3), 34001 (2023) <https://doi.org/10.1209/0295-5075/ace7f0> arXiv:2307.08842 [hep-ph]
- [17] Barranco, J., Miranda, O.G., Rashba, T.I.: Probing new physics with coherent neutrino scattering off nuclei. JHEP **12**, 021 (2005) <https://doi.org/10.1088/1126-6708/2005/12/021> arXiv:hep-ph/0508299
- [18] Billard, J., Johnston, J., Kavanagh, B.J.: Prospects for exploring New Physics in Coherent Elastic Neutrino-Nucleus Scattering. JCAP **11**, 016 (2018) <https://doi.org/10.1088/1475-7516/2018/11/016> arXiv:1805.01798 [hep-ph]
- [19] Cadeddu, M., Giunti, C., Kouzakov, K.A., Li, Y.-F., Zhang, Y.-Y., Studenikin, A.I.: Neutrino Charge Radii From Coherent Elastic Neutrino-nucleus Scattering. Phys. Rev. D **98**(11), 113010 (2018) https://doi.org/10.1142/9789811233913_0013 arXiv:1810.05606 [hep-ph]. [Erratum: Phys.Rev.D 101, 059902 (2020)]
- [20] Wolfenstein, L.: Neutrino Oscillations in Matter. Phys. Rev. D **17**, 2369–2374 (1978) <https://doi.org/10.1103/PhysRevD.17.2369>
- [21] Ohlsson, T.: Status of non-standard neutrino interactions. Rept. Prog. Phys. **76**, 044201 (2013) <https://doi.org/10.1088/0034-4885/76/4/044201> arXiv:1209.2710 [hep-ph]
- [22] Bhupal Dev, P.S., *et al.*: Neutrino non-standard interactions: A status report. SciPost Phys. Proc., 001 (2019) <https://doi.org/10.21468/SciPostPhysProc.2.001>
- [23] Giunti, C., Studenikin, A.: Neutrino electromagnetic interactions: a window to new physics. Rev. Mod. Phys. **87**, 531 (2015) <https://doi.org/10.1103/RevModPhys.87.531> arXiv:1403.6344 [hep-ph]
- [24] Bonet, H., *et al.*: Constraints on elastic neutrino nucleus scattering in the fully coherent regime from the CONUS experiment. Phys. Rev. Lett. **126**(4), 041804 (2021) <https://doi.org/10.1103/PhysRevLett.126.041804> arXiv:2011.00210 [hep-ex]
- [25] Aguilar-Arevalo, A., *et al.*: The CONNIE experiment. J. Phys. Conf. Ser. **761**(1), 012057 (2016) <https://doi.org/10.1088/1742-6596/761/1/012057> arXiv:1608.01565 [physics.ins-det]
- [26] Akimov, D., *et al.*: The COHERENT Experimental Program. arXiv e-prints, 2204–04575 (2022) <https://doi.org/10.48550/arXiv.2204.04575> arXiv:2204.04575 [hep-ex]
- [27] Agnolet, G., *et al.*: Background Studies for the MINER Coherent Neutrino Scattering

- Reactor Experiment. Nucl. Instrum. Meth. A **853**, 53–60 (2017) <https://doi.org/10.1016/j.nima.2017.02.024> arXiv:1609.02066 [physics.ins-det]
- [28] Choi, J.J., *et al.*: Exploring coherent elastic neutrino-nucleus scattering using reactor electron antineutrinos in the NEON experiment. Eur. Phys. J. C **83**(3), 226 (2023) <https://doi.org/10.1140/epjc/s10052-023-11352-x> arXiv:2204.06318 [hep-ex]
- [29] Angloher, G., *et al.*: Exploring CE ν NS with NUCLEUS at the Chooz nuclear power plant. Eur. Phys. J. C **79**(12), 1018 (2019) <https://doi.org/10.1140/epjc/s10052-019-7454-4> arXiv:1905.10258 [physics.ins-det]
- [30] Colas, J., Billard, J., Ferriol, S., Gascon, J., Salagnac, T.: Development of Data Processing and Analysis Pipeline for the Ricochet Experiment. J. Low Temp. Phys. **211**(5-6), 310–319 (2023) <https://doi.org/10.1007/s10909-022-02907-5> arXiv:2111.12856 [physics.ins-det]
- [31] Akimov, D.Y., *et al.*: The RED-100 experiment. JINST **17**(11), 11011 (2022) <https://doi.org/10.1088/1748-0221/17/11/T11011> arXiv:2209.15516 [physics.ins-det]
- [32] Baxter, D., *et al.*: Coherent Elastic Neutrino-Nucleus Scattering at the European Spallation Source. JHEP **02**, 123 (2020) [https://doi.org/10.1007/JHEP02\(2020\)123](https://doi.org/10.1007/JHEP02(2020)123) arXiv:1911.00762 [physics.ins-det]
- [33] Cañas, B.C., Garcés, E.A., Miranda, O.G., Parada, A.: Future perspectives for a weak mixing angle measurement in coherent elastic neutrino nucleus scattering experiments. Phys. Lett. B **784**, 159–162 (2018) <https://doi.org/10.1016/j.physletb.2018.07.049> arXiv:1806.01310 [hep-ph]
- [34] Hirata, K., *et al.*: Observation of a Neutrino Burst from the Supernova SN 1987a. Phys. Rev. Lett. **58**, 1490–1493 (1987) <https://doi.org/10.1103/PhysRevLett.58.1490>
- [35] Haines, T., *et al.*: Neutrinos From SN1987A in the Imb Detector. Nucl. Instrum. Meth. A **264**, 28–31 (1988) [https://doi.org/10.1016/0168-9002\(88\)91097-2](https://doi.org/10.1016/0168-9002(88)91097-2)
- [36] Alekseev, E.N., Alekseeva, L.N., Krivosheina, I.V., Volchenko, V.I.: Properties of the Supernova 1987A Neutrino Signal Recorded by the Baksan Underground Scintillation Telescope. Soviet Astronomy Letters **14**, 41 (1988)
- [37] Hudepohl, L.: Neutrinos from the Formation, Cooling and Black Hole Collapse of Neutron Stars. PhD thesis, Munich, Tech. U. (October 2013)
- [38] Mirizzi, A., Tamborra, I., Janka, H.-T., Saviano, N., Scholberg, K., Bollig, R., Hudepohl, L., Chakraborty, S.: Supernova Neutrinos: Production, Oscillations and Detection. Riv. Nuovo Cim. **39**(1-2), 1–112 (2016) <https://doi.org/10.1393/ncr/i2016-10120-8> arXiv:1508.00785 [astro-ph.HE]
- [39] Nagakura, H., Burrows, A., Vartanyan, D., Radice, D.: Core-collapse supernova neutrino emission and detection informed by state-of-the-art three-dimensional numerical models. Mon. Not. Roy. Astron. Soc. **500**(1), 696–717 (2020) <https://doi.org/10.1093/mnras/staa2691> arXiv:2007.05000 [astro-ph.HE]
- [40] Burrows, A., Vartanyan, D.: Core-Collapse Supernova Explosion Theory. Nature **589**(7840), 29–39 (2021) <https://doi.org/10.1038/s41586-020-03059-w> arXiv:2009.14157 [astro-ph.SR]
- [41] Lang, R.F., McCabe, C., Reichard, S., Selvi, M., Tamborra, I.: Supernova neutrino physics with xenon dark matter detectors: A timely perspective. Phys. Rev. D **94**(10), 103009 (2016) <https://doi.org/10.1103/PhysRevD.94.103009> arXiv:1606.09243 [astro-ph.HE]
- [42] Agnes, P., *et al.*: Sensitivity of future liquid argon dark matter search experiments to core-collapse supernova

- neutrinos. JCAP **03**, 043 (2021) <https://doi.org/10.1088/1475-7516/2021/03/043> arXiv:2011.07819 [astro-ph.HE]
- [43] Abe, K., *et al.*: Real-Time Supernova Neutrino Burst Monitor at Super-Kamiokande. *Astropart. Phys.* **81**, 39–48 (2016) <https://doi.org/10.1016/j.astropartphys.2016.04.003> arXiv:1601.04778 [astro-ph.HE]
- [44] Abe, K., *et al.*: Supernova Model Discrimination with Hyper-Kamiokande. *Astrophys. J.* **916**(1), 15 (2021) <https://doi.org/10.3847/1538-4357/abf7c4> arXiv:2101.05269 [astro-ph.IM]
- [45] Abi, B., *et al.*: Supernova neutrino burst detection with the Deep Underground Neutrino Experiment. *Eur. Phys. J. C* **81**(5), 423 (2021) <https://doi.org/10.1140/epjc/s10052-021-09166-w> arXiv:2008.06647 [hep-ex]
- [46] Pattavina, L., Ferreiro Iachellini, N., Tamborra, I.: Neutrino observatory based on archaeological lead. *Phys. Rev. D* **102**(6), 063001 (2020) <https://doi.org/10.1103/PhysRevD.102.063001> arXiv:2004.06936 [astro-ph.HE]
- [47] Pattavina, L., *et al.*: RES-NOVA sensitivity to core-collapse and failed core-collapse supernova neutrinos. JCAP **10**, 064 (2021) <https://doi.org/10.1088/1475-7516/2021/10/064> arXiv:2103.08672 [astro-ph.IM]
- [48] Abusleme, A., *et al.*: JUNO physics and detector. *Prog. Part. Nucl. Phys.* **123**, 103927 (2022) <https://doi.org/10.1016/j.ppnp.2021.103927> arXiv:2104.02565 [hep-ex]
- [49] Scholberg, K.: Supernova Neutrino Detection. *Ann. Rev. Nucl. Part. Sci.* **62**, 81–103 (2012) <https://doi.org/10.1146/annurev-nucl-102711-095006> arXiv:1205.6003 [astro-ph.IM]
- [50] Horiuchi, S., Kneller, J.P.: What can be learned from a future supernova neutrino detection? *J. Phys. G* **45**(4), 043002 (2018) <https://doi.org/10.1088/1361-6471/aaa90a> arXiv:1709.01515 [astro-ph.HE]
- [51] Nikrant, A., Laha, R., Horiuchi, S.: Robust measurement of supernova ν_e spectra with future neutrino detectors. *Phys. Rev. D* **97**(2), 023019 (2018) <https://doi.org/10.1103/PhysRevD.97.023019> arXiv:1711.00008 [astro-ph.HE]
- [52] Gallo Rosso, A., Vissani, F., Volpe, M.C.: What can we learn on supernova neutrino spectra with water Cherenkov detectors? JCAP **04**, 040 (2018) <https://doi.org/10.1088/1475-7516/2018/04/040> arXiv:1712.05584 [hep-ph]
- [53] Li, H.-L., Li, Y.-F., Wang, M., Wen, L.-J., Zhou, S.: Towards a complete reconstruction of supernova neutrino spectra in future large liquid-scintillator detectors. *Phys. Rev. D* **97**(6), 063014 (2018) <https://doi.org/10.1103/PhysRevD.97.063014> arXiv:1712.06985 [hep-ph]
- [54] Li, H.-L., Huang, X., Li, Y.-F., Wen, L.-J., Zhou, S.: Model-independent approach to the reconstruction of multiflavor supernova neutrino energy spectra. *Phys. Rev. D* **99**(12), 123009 (2019) <https://doi.org/10.1103/PhysRevD.99.123009> arXiv:1903.04781 [hep-ph]
- [55] Nagakura, H.: Retrieval of energy spectra for all flavours of neutrinos from core-collapse supernova with multiple detectors. *Mon. Not. Roy. Astron. Soc.* **500**(1), 319–332 (2020) <https://doi.org/10.1093/mnras/staa3287> arXiv:2008.10082 [astro-ph.HE]
- [56] Huang, X.-R., Sun, C.-L., Chen, L.-W., Gao, J.: Bayesian inference of supernova neutrino spectra with multiple detectors. JCAP **09**, 040 (2023) <https://doi.org/10.1088/1475-7516/2023/09/040> arXiv:2305.00392 [hep-ph]
- [57] Aalseth, C.E., *et al.*: DarkSide-20k: A 20 tonne two-phase LAr TPC for direct dark matter detection at LNGS. *Eur. Phys. J. Plus* **133**, 131 (2018) <https://doi.org/10.1140/epjp/i2018-11973-4> arXiv:1707.08145 [physics.ins-det]

- [58] Müller, B.: The Status of Multi-Dimensional Core-Collapse Supernova Models. *Publ. Astron. Soc. Austral.* **33**, 048 (2016) <https://doi.org/10.1017/pasa.2016.40> [arXiv:1608.03274](https://arxiv.org/abs/1608.03274) [astro-ph.SR]
- [59] Keil, M.T., Raffelt, G.G., Janka, H.-T.: Monte Carlo study of supernova neutrino spectra formation. *Astrophys. J.* **590**, 971–991 (2003) <https://doi.org/10.1086/375130> [arXiv:astro-ph/0208035](https://arxiv.org/abs/astro-ph/0208035)
- [60] Tamborra, I., Müller, B., Hudepohl, L., Janka, H.-T., Raffelt, G.: High-resolution supernova neutrino spectra represented by a simple fit. *Phys. Rev. D* **86**, 125031 (2012) <https://doi.org/10.1103/PhysRevD.86.125031> [arXiv:1211.3920](https://arxiv.org/abs/1211.3920) [astro-ph.SR]
- [61] Scholberg, K.: Supernova Signatures of Neutrino Mass Ordering. *J. Phys. G* **45**(1), 014002 (2018) <https://doi.org/10.1088/1361-6471/aa97be> [arXiv:1707.06384](https://arxiv.org/abs/1707.06384) [hep-ex]
- [62] O’Connor, E., Ott, C.D.: The Progenitor Dependence of the Preexplosion Neutrino Emission in Core-Collapse Supernovae. *Astrophys. J.* **762**, 126 (2013) <https://doi.org/10.1088/0004-637X/762/2/126> [arXiv:1207.1100](https://arxiv.org/abs/1207.1100) [astro-ph.HE]
- [63] Seadrow, S., Burrows, A., Vartanyan, D., Radice, D., Skinner, M.A.: Neutrino Signals of Core-Collapse Supernovae in Underground Detectors. *Mon. Not. Roy. Astron. Soc.* **480**(4), 4710–4731 (2018) <https://doi.org/10.1093/mnras/sty2164> [arXiv:1804.00689](https://arxiv.org/abs/1804.00689) [astro-ph.HE]
- [64] Pan, K.-C., Liebendörfer, M., Couch, S.M., Thielemann, F.-K.: Equation of State Dependent Dynamics and Multimessenger Signals from Stellar-mass Black Hole Formation. *Astrophys. J.* **857**(1), 13 (2018) <https://doi.org/10.3847/1538-4357/aab71d> [arXiv:1710.01690](https://arxiv.org/abs/1710.01690) [astro-ph.HE]
- [65] Silva Schneider, A., O’Connor, E., Granqvist, E., Betranhandy, A., Couch, S.M.: Equation of State and Progenitor Dependence of Stellar-mass Black Hole Formation. *Astrophys. J.* **894**(1), 4 (2020) <https://doi.org/10.3847/1538-4357/ab8308> [arXiv:2001.10434](https://arxiv.org/abs/2001.10434) [astro-ph.HE]
- [66] Raduta, A.R., Nacu, F., Oertel, M.: Equations of state for hot neutron stars. *Eur. Phys. J. A* **57**(12), 329 (2021) <https://doi.org/10.1140/epja/s10050-021-00628-z> [arXiv:2109.00251](https://arxiv.org/abs/2109.00251) [nucl-th]
- [67] Marrodán Undagoitia, T., Rauch, L.: Dark matter direct-detection experiments. *J. Phys. G* **43**(1), 013001 (2016) <https://doi.org/10.1088/0954-3899/43/1/013001> [arXiv:1509.08767](https://arxiv.org/abs/1509.08767) [physics.ins-det]
- [68] O’Hare, C.A.J.: New Definition of the Neutrino Floor for Direct Dark Matter Searches. *Phys. Rev. Lett.* **127**(25), 251802 (2021) <https://doi.org/10.1103/PhysRevLett.127.251802> [arXiv:2109.03116](https://arxiv.org/abs/2109.03116) [hep-ph]
- [69] Khaitan, D.: Supernova neutrino detection in LZ. *JINST* **13**(02), 02024 (2018) <https://doi.org/10.1088/1748-0221/13/02/C02024> [arXiv:1801.05651](https://arxiv.org/abs/1801.05651)
- [70] Drukier, A., Stodolsky, L.: Principles and Applications of a Neutral Current Detector for Neutrino Physics and Astronomy. *Phys. Rev. D* **30**, 2295 (1984) <https://doi.org/10.1103/PhysRevD.30.2295>
- [71] Lindner, M., Rodejohann, W., Xu, X.-J.: Coherent Neutrino-Nucleus Scattering and new Neutrino Interactions. *JHEP* **03**, 097 (2017) [https://doi.org/10.1007/JHEP03\(2017\)097](https://doi.org/10.1007/JHEP03(2017)097) [arXiv:1612.04150](https://arxiv.org/abs/1612.04150) [hep-ph]
- [72] Huang, X.-R., Chen, L.-W.: Supernova neutrinos as a precise probe of nuclear neutron skin. *Phys. Rev. D* **106**(12), 123034 (2022) <https://doi.org/10.1103/PhysRevD.106.123034> [arXiv:2210.04534](https://arxiv.org/abs/2210.04534) [nucl-th]
- [73] Meija, J., Coplen, T.B., Berglund, M., Brand, W.A., Bièvre, P.D., Gröning, M., Holden, N.E., Irrgeher, J., Loss, R.D., Walczyk, T., Prohaska, T.: Isotopic compositions of the elements 2013 (iupac technical report). *Pure and Applied Chemistry*

- 88**(3), 293–306 (2016) <https://doi.org/10.1515/pac-2015-0503>
- [74] Wang, M., Huang, W.J., Kondev, F.G., Audi, G., Naimi, S.: The AME 2020 atomic mass evaluation (II). Tables, graphs and references. *Chin. Phys. C* **45**(3), 030003 (2021) <https://doi.org/10.1088/1674-1137/abddaf>
- [75] Helm, R.H.: Inelastic and Elastic Scattering of 187-Mev Electrons from Selected Even-Even Nuclei. *Phys. Rev.* **104**, 1466–1475 (1956) <https://doi.org/10.1103/PhysRev.104.1466>
- [76] Piekarewicz, J., Linero, A.R., Giuliani, P., Chicken, E.: Power of two: Assessing the impact of a second measurement of the weak-charge form factor of ^{208}Pb . *Phys. Rev. C* **94**(3), 034316 (2016) <https://doi.org/10.1103/PhysRevC.94.034316> [arXiv:1604.07799](https://arxiv.org/abs/1604.07799) [nucl-th]
- [77] Rosen, M., Raphael, R., Überall, H.: Generalized helm model for transverse electroexcitation of nuclear levels. *Phys. Rev.* **163**, 927–934 (1967) <https://doi.org/10.1103/PhysRev.163.927>
- [78] Raphael, R., Rosen, M.: Electron Scattering from Deformed Nuclei. *Phys. Rev. C* **1**, 547–560 (1970) <https://doi.org/10.1103/PhysRevC.1.547>
- [79] Friedrich, J., Voegler, N.: The salient features of charge density distributions of medium and heavy even-even nuclei determined from a systematic analysis of elastic electron scattering form factors. *Nucl. Phys. A* **373**, 192–224 (1982) [https://doi.org/10.1016/0375-9474\(82\)90147-6](https://doi.org/10.1016/0375-9474(82)90147-6)
- [80] Cadeddu, M., Giunti, C., Li, Y.F., Zhang, Y.Y.: Average CsI neutron density distribution from COHERENT data. *Phys. Rev. Lett.* **120**(7), 072501 (2018) <https://doi.org/10.1103/PhysRevLett.120.072501> [arXiv:1710.02730](https://arxiv.org/abs/1710.02730) [hep-ph]
- [81] Huang, X.-R., Chen, L.-W.: Neutron Skin in CsI and Low-Energy Effective Weak Mixing Angle from COHERENT Data. *Phys. Rev. D* **100**(7), 071301 (2019) <https://doi.org/10.1103/PhysRevD.100.071301> [arXiv:1902.07625](https://arxiv.org/abs/1902.07625) [hep-ph]
- [82] Cadeddu, M., Dordei, F., Giunti, C., Li, Y.F., Picciau, E., Zhang, Y.Y.: Physics results from the first COHERENT observation of coherent elastic neutrino-nucleus scattering in argon and their combination with cesium-iodide data. *Phys. Rev. D* **102**(1), 015030 (2020) <https://doi.org/10.1103/PhysRevD.102.015030> [arXiv:2005.01645](https://arxiv.org/abs/2005.01645) [hep-ph]
- [83] Hammer, H.-W., Meißner, U.-G.: The proton radius: From a puzzle to precision. *Sci. Bull.* **65**, 257–258 (2020) <https://doi.org/10.1016/j.scib.2019.12.012> [arXiv:1912.03881](https://arxiv.org/abs/1912.03881) [hep-ph]
- [84] Tanabashi, M., *et al.*: Review of Particle Physics. *Phys. Rev. D* **98**(3), 030001 (2018) <https://doi.org/10.1103/PhysRevD.98.030001>
- [85] Ong, A., Berengut, J.C., Flambaum, V.V.: The Effect of spin-orbit nuclear charge density corrections due to the anomalous magnetic moment on halonuclei. *Phys. Rev. C* **82**, 014320 (2010) <https://doi.org/10.1103/PhysRevC.82.014320> [arXiv:1006.5508](https://arxiv.org/abs/1006.5508) [nucl-th]
- [86] Horowitz, C.J., *et al.*: Weak charge form factor and radius of ^{208}Pb through parity violation in electron scattering. *Phys. Rev. C* **85**, 032501 (2012) <https://doi.org/10.1103/PhysRevC.85.032501> [arXiv:1202.1468](https://arxiv.org/abs/1202.1468) [nucl-ex]
- [87] Fricke, G., Bernhardt, C., Heilig, K., Schaller, L.A., Schellenberg, L., Shera, E.B., Jager, C.W.: Nuclear Ground State Charge Radii from Electromagnetic Interactions. *Atom. Data Nucl. Data Tabl.* **60**, 177–285 (1995) <https://doi.org/10.1006/adnd.1995.1007>
- [88] Angeli, I., Marinova, K.P.: Table of experimental nuclear ground state charge radii: An update. *Atom. Data Nucl. Data Tabl.* **99**(1), 69–95 (2013) <https://doi.org/10.1016/j.adt>

2011.12.006

- [89] Thiel, M., Sfienti, C., Piekarewicz, J., Horowitz, C.J., Vanderhaeghen, M.: Neutron skins of atomic nuclei: per aspera ad astra. *J. Phys. G* **46**(9), 093003 (2019) <https://doi.org/10.1088/1361-6471/ab2c6d> arXiv:1904.12269 [nucl-ex]
- [90] Agnes, P., *et al.*: Low-Mass Dark Matter Search with the DarkSide-50 Experiment. *Phys. Rev. Lett.* **121**(8), 081307 (2018) <https://doi.org/10.1103/PhysRevLett.121.081307> arXiv:1802.06994 [astro-ph.HE]
- [91] Agnes, P., *et al.*: Electroluminescence pulse shape and electron diffusion in liquid argon measured in a dual-phase TPC. *Nucl. Instrum. Meth. A* **904**, 23–34 (2018) <https://doi.org/10.1016/j.nima.2018.06.077> arXiv:1802.01427 [physics.ins-det]
- [92] Navas, S., *et al.*: Review of particle physics. *Phys. Rev. D* **110**(3), 030001 (2024) <https://doi.org/10.1103/PhysRevD.110.030001>
- [93] Bresó-Pla, V., Falkowski, A., González-Alonso, M., Monsálvez-Pozo, K.: EFT analysis of New Physics at COHERENT. *JHEP* **05**, 074 (2023) [https://doi.org/10.1007/JHEP05\(2023\)074](https://doi.org/10.1007/JHEP05(2023)074) arXiv:2301.07036 [hep-ph]
- [94] Davidson, S., Pena-Garay, C., Rius, N., Santamaria, A.: Present and future bounds on nonstandard neutrino interactions. *JHEP* **03**, 011 (2003) <https://doi.org/10.1088/1126-6708/2003/03/011> arXiv:hep-ph/0302093
- [95] Scholberg, K.: Prospects for measuring coherent neutrino-nucleus elastic scattering at a stopped-pion neutrino source. *Phys. Rev. D* **73**, 033005 (2006) <https://doi.org/10.1103/PhysRevD.73.033005> arXiv:hep-ex/0511042
- [96] Coloma, P., Denton, P.B., Gonzalez-Garcia, M.C., Maltoni, M., Schwetz, T.: Curtailing the Dark Side in Non-Standard Neutrino Interactions. *JHEP* **04**, 116 (2017) [https://doi.org/10.1007/JHEP04\(2017\)116](https://doi.org/10.1007/JHEP04(2017)116) arXiv:1701.04828 [hep-ph]
- [97] Papoulias, D.K., Kosmas, T.S.: COHERENT constraints to conventional and exotic neutrino physics. *Phys. Rev. D* **97**(3), 033003 (2018) <https://doi.org/10.1103/PhysRevD.97.033003> arXiv:1711.09773 [hep-ph]
- [98] Coloma, P., Gonzalez-Garcia, M.C., Maltoni, M., Schwetz, T.: COHERENT Enlightenment of the Neutrino Dark Side. *Phys. Rev. D* **96**(11), 115007 (2017) <https://doi.org/10.1103/PhysRevD.96.115007> arXiv:1708.02899 [hep-ph]
- [99] Khan, A.N., Rodejohann, W.: New physics from COHERENT data with an improved quenching factor. *Phys. Rev. D* **100**(11), 113003 (2019) <https://doi.org/10.1103/PhysRevD.100.113003> arXiv:1907.12444 [hep-ph]
- [100] Papoulias, D.K.: COHERENT constraints after the COHERENT-2020 quenching factor measurement. *Phys. Rev. D* **102**(11), 113004 (2020) <https://doi.org/10.1103/PhysRevD.102.113004> arXiv:1907.11644 [hep-ph]
- [101] Giunti, C.: General COHERENT constraints on neutrino nonstandard interactions. *Phys. Rev. D* **101**(3), 035039 (2020) <https://doi.org/10.1103/PhysRevD.101.035039> arXiv:1909.00466 [hep-ph]
- [102] Mukhopadhyay, M., Lunardini, C., Timmes, F.X., Zuber, K.: Presupernova neutrinos: directional sensitivity and prospects for progenitor identification. *Astrophys. J.* **899**(2), 153 (2020) <https://doi.org/10.3847/1538-4357/ab99a6> arXiv:2004.02045 [astro-ph.HE]
- [103] Pledger, J.L., Shara, M.M.: Possible Detection of the Progenitor of the Type II Supernova SN 2023ixf. *Astrophys. J. Lett.* **953**(1), 14 (2023) <https://doi.org/10.3847/2041-8213/ace88b> arXiv:2305.14447 [astro-ph.SR]

- [104] Fiorella Burgio, G., Fantina, A.F.: Nuclear Equation of state for Compact Stars and Supernovae. *Astrophys. Space Sci. Libr.* **457**, 255–335 (2018) https://doi.org/10.1007/978-3-319-97616-7_6 [arXiv:1804.03020](https://arxiv.org/abs/1804.03020) [nucl-th]
- [105] Burgio, G.F., Schulze, H.-J., Vidana, I., Wei, J.-B.: Neutron stars and the nuclear equation of state. *Prog. Part. Nucl. Phys.* **120**, 103879 (2021) <https://doi.org/10.1016/j.pnpnp.2021.103879> [arXiv:2105.03747](https://arxiv.org/abs/2105.03747) [nucl-th]
- [106] Lattimer, J.M.: Neutron Stars and the Nuclear Matter Equation of State. *Ann. Rev. Nucl. Part. Sci.* **71**, 433–464 (2021) <https://doi.org/10.1146/annurev-nucl-102419-124827>
- [107] Youngblood, D.H., Clark, H.L., Lui, Y.-W.: Incompressibility of Nuclear Matter from the Giant Monopole Resonance. *Phys. Rev. Lett.* **82**, 691–694 (1999) <https://doi.org/10.1103/PhysRevLett.82.691>
- [108] Shlomo, S., Kolomietz, V.M., Colò, G.: Deducing the nuclear-matter incompressibility coefficient from data on isoscalar compression modes. *Eur. Phys. J. A* **30**(1), 23–30 (2006) <https://doi.org/10.1140/epja/i2006-10100-3>
- [109] Chen, L.-W., Gu, J.-Z.: Correlations between the nuclear breathing mode energy and properties of asymmetric nuclear matter. *J. Phys. G* **39**, 035104 (2012) <https://doi.org/10.1088/0954-3899/39/3/035104> [arXiv:1104.5407](https://arxiv.org/abs/1104.5407) [nucl-th]
- [110] Colo, G., Garg, U., Sagawa, H.: Symmetry energy from the nuclear collective motion: constraints from dipole, quadrupole, monopole and spin-dipole resonances. *Eur. Phys. J. A* **50**, 26 (2014) <https://doi.org/10.1140/epja/i2014-14026-9> [arXiv:1309.1572](https://arxiv.org/abs/1309.1572) [nucl-th]
- [111] Garg, U., Colò, G.: The compression-mode giant resonances and nuclear incompressibility. *Prog. Part. Nucl. Phys.* **101**, 55–95 (2018) <https://doi.org/10.1016/j.pnpnp.2018.03.001> [arXiv:1801.03672](https://arxiv.org/abs/1801.03672) [nucl-ex]
- [112] Cai, B.-J., Li, B.-A.: Auxiliary function approach for determining symmetry energy at suprasaturation densities. *Phys. Rev. C* **103**(5), 054611 (2021) <https://doi.org/10.1103/PhysRevC.103.054611> [arXiv:2104.02185](https://arxiv.org/abs/2104.02185) [nucl-th]
- [113] Li, B.-A., Cai, B.-J., Xie, W.-J., Zhang, N.-B.: Progress in Constraining Nuclear Symmetry Energy Using Neutron Star Observables Since GW170817. *Universe* **7**(6), 182 (2021) <https://doi.org/10.3390/universe7060182> [arXiv:2105.04629](https://arxiv.org/abs/2105.04629) [nucl-th]
- [114] Lattimer, J.M., Swesty, F.D.: A Generalized equation of state for hot, dense matter. *Nucl. Phys. A* **535**, 331–376 (1991) [https://doi.org/10.1016/0375-9474\(91\)90452-C](https://doi.org/10.1016/0375-9474(91)90452-C)
- [115] Shen, H., Toki, H., Oyamatsu, K., Sumiyoshi, K.: Relativistic equation of state of nuclear matter for supernova and neutron star. *Nucl. Phys. A* **637**, 435–450 (1998) [https://doi.org/10.1016/S0375-9474\(98\)00236-X](https://doi.org/10.1016/S0375-9474(98)00236-X) [arXiv:nuc1-th/9805035](https://arxiv.org/abs/nuc1-th/9805035)
- [116] Leifels, Y., LeFevre, A., Reisdorf, W., Aichelelin, J., Hartnack, C.: Constraining the nuclear matter equation of state around twice saturation density. *EPJ Web Conf.* **88**, 00018 (2015) <https://doi.org/10.1051/epjconf/20158800018>
- [117] Huth, S., *et al.*: Constraining Neutron-Star Matter with Microscopic and Macroscopic Collisions. *Nature* **606**, 276–280 (2022) <https://doi.org/10.1038/s41586-022-04750-w> [arXiv:2107.06229](https://arxiv.org/abs/2107.06229) [nucl-th]
- [118] Sorensen, A., *et al.*: Dense nuclear matter equation of state from heavy-ion collisions. *Prog. Part. Nucl. Phys.* **134**, 104080 (2024) <https://doi.org/10.1016/j.pnpnp.2023.104080> [arXiv:2301.13253](https://arxiv.org/abs/2301.13253) [nucl-th]
- [119] Raaijmakers, G., Greif, S.K., Hebeler, K., Hinderer, T., Nissanke, S., Schwenk, A., Riley, T.E., Watts, A.L., Lattimer, J.M., Ho,

- W.C.G.: Constraints on the Dense Matter Equation of State and Neutron Star Properties from NICER’s Mass–Radius Estimate of PSR J0740+6620 and Multimessenger Observations. *Astrophys. J. Lett.* **918**(2), 29 (2021) <https://doi.org/10.3847/2041-8213/ac089a> arXiv:2105.06981 [astro-ph.HE]
- [120] Zhang, N.-B., Li, B.-A.: Impact of NICER’s Radius Measurement of PSR J0740+6620 on Nuclear Symmetry Energy at Suprasaturation Densities. *Astrophys. J.* **921**(2), 111 (2021) <https://doi.org/10.3847/1538-4357/ac1e8c> arXiv:2105.11031 [nucl-th]
- [121] Pang, P.T.H., Tews, I., Coughlin, M.W., Bulla, M., Van Den Broeck, C., Dietrich, T.: Nuclear Physics Multimessenger Astrophysics Constraints on the Neutron Star Equation of State: Adding NICER’s PSR J0740+6620 Measurement. *Astrophys. J.* **922**(1), 14 (2021) <https://doi.org/10.3847/1538-4357/ac19ab> arXiv:2105.08688 [astro-ph.HE]
- [122] Radice, D., Perego, A., Zappa, F., Bernuzzi, S.: GW170817: Joint Constraint on the Neutron Star Equation of State from Multimessenger Observations. *Astrophys. J. Lett.* **852**(2), 29 (2018) <https://doi.org/10.3847/2041-8213/aaa402> arXiv:1711.03647 [astro-ph.HE]
- [123] Abbott, B.P., *et al.*: Properties of the binary neutron star merger GW170817. *Phys. Rev. X* **9**(1), 011001 (2019) <https://doi.org/10.1103/PhysRevX.9.011001> arXiv:1805.11579 [gr-qc]
- [124] Rozwadowska, K., Vissani, F., Cappelaro, E.: On the rate of core collapse supernovae in the milky way. *New Astron.* **83**, 101498 (2021) <https://doi.org/10.1016/j.newast.2020.101498> arXiv:2009.03438 [astro-ph.HE]
- [125] Bethe, H.A.: Supernova mechanisms. *Rev. Mod. Phys.* **62**, 801–866 (1990) <https://doi.org/10.1103/RevModPhys.62.801>
- [126] The, L.-S., Clayton, D.D., Diehl, R., Hartmann, D.H., Iyudin, A.F., Leising, M.D., Meyer, B.S., Motizuki, Y., Schonfelder, V.: Are ti-44 producing supernovae exceptional? *Astron. Astrophys.* **450**, 1037 (2006) <https://doi.org/10.1051/0004-6361:20054626> arXiv:astro-ph/0601039
- [127] Cao, X., *et al.*: PandaX: A Liquid Xenon Dark Matter Experiment at CJPL. *Sci. China Phys. Mech. Astron.* **57**, 1476–1494 (2014) <https://doi.org/10.1007/s11433-014-5521-2> arXiv:1405.2882 [physics.ins-det]
- [128] Aprile, E., *et al.*: The XENONnT dark matter experiment. *Eur. Phys. J. C* **84**(8), 784 (2024) <https://doi.org/10.1140/epjc/s10052-024-12982-5> arXiv:2402.10446 [physics.ins-det]